MINERALOGIA POLONICA
Vol. 13, No 1 — 1982

*Tadeusz WIESER**

MANGANIFEROUS CARBONATE MICRONODULES OF THE POLISH CARPATHIANS FLYSCH DEPOSITS AND THEIR ORIGIN

UKD 552.124.4:546.711'246].08:552.52'542.08:551.263.23:551.781(438-13-924.51)

Abstract. The chemical constitution of Palaeogene Flysch clayey and marly sediments combined with environmental conditions during and after deposition were the leading factors responsible for peculiar composition and physiography of the examined carbonate micronodules. The mineral composition of carbonates varies between rhodochrosite, oligonite nad Ca-rhodochrosite, as in the bulk of Carpathian Flysch macronodules, not without influence on the shape and structure of micronodules, accordingly. The paucity in trace elements and low C^{13}/C^{12} ratio in investigated Mn-rich carbonates are interpreted in terms of low crystal lattice tolerance for substitution and high participation of enzymic (bacterial) decarboxylation processes of organic compounds, respectively. Diagenetic and hydrogeneous (precipitation from pore waters) origin of micronodules is postulated and the main source of manganese is involved in the hydrolytic decomposition, of volcanic glass. Decaying, abnormally abundant organic matter favoured decomposition, mobilization, ascenzional migration, while for precipitation and growth decided less reducing environment created in overlying sediments of bottom surface neighbourhood.

INTRODUCTION

Fossil deep-sea manganese macronodules are exceptionally scarse in the marine sediments accessible for study on lands. After Jenkyns's (1977) record the list of occurrences embraces Indonesian Archipelago, the Alpine Mediterranean, Washington State (USA), Barbados and Sicily only, ranging in age from Jurassic to Miocene. Even if supplemented by corresponding (oxyhydroxide) ferromanganese macronodules found in the Palaeogene to Cretaceous Carpathian Flysch deposits of Poland/ /(Gucwa and Wieser, 1978), the paucity of published examples appears remarkable.

The approximate distribution of manganese macronodules in the actual oceanic areas by age may be evaluated after Glasby's (1978) data (in per cents, basing on 51 holes), as follows: Pleistocene — 42, Pliocene — 7, Miocene — 21, Oligocene — 9, Eocene — 11, Palaeocene — 2, Cretaceous — 6 and Jurassic — 2.

The fossil manganiferous micronodules are much more rarely reported beyond actual oceanic areas. The only well known occurrence is that investigated by Molengraaff (1921) and later by El Wakeel and Riley (1961), localized in Cretaceous red clays of Timor Island. As in the macronodule case this is not valid for fossil mangani-

* Carpathian Division, Geological Institute, Cracow (31-560 Kraków, ul. Skrzatów 1).

ferous micronodules confined to the deposits of present oceans. Glasby (1978) tabulates all the examples provided by DSDP borings, announcing the presence of Upper Miocene to Oligocene micronodules in Pacific and Atlantic zeolitic pelagic clays, as well as in biosiliceous oozes and biosiliceous silty clays. For comparison reasons let us mention, that the above cited micronodules occurred in sediments a little different to those containing macronodules. Glasby (op. cit.) gives for the last mentioned following distribution percentage: pelagic clays — 60, calcareous ooze — 30, siliceous ooze — 8, sand and gravel — 2.

Other fossil micronodule findings among oceanic deposits include, for example, carbonate ones. Fe-rhodochrosite or Mn-siderite microconcretions were lately discovered by Kossovskaya and Dritz (1979) in montmorillonitic sediment of Oligocene-Miocene age. In the North Atlantic were also cored sediments rich in globules of Mn-calcite and pyrite of Eocene age (Varentsov and Dritz, 1979).

Chester and Hughes (1969) induce striking statement postulating that among manganese nodule-bearing pelagic clays of a North Pacific core about 80—90 per cent of the total Mn content in sediment (varying from 0.43 to 0.82 per cent MnO) has a hydrogeneous origin and of this nearly 85 per cent is associated with the micronodules, dispersed throughout the sediment.

Stackelberg (1979) observed that in Northern Central Pacific micronodules existed mainly in Early Miocene and Late Pliocene sediments, being particularly concentrated near the hiatus between cited chronostratigraphic units. This remains in accordance with Margolis's (fide Stackelberg, 1979) conclusion pointing out low rates of sedimentation and oxygen-rich bottom currents as favouring factors. In the case of carbonate manganiferous micronodules the second factor could be only destructive, through replacement by Mn-oxide or-hydroxide compounds.

Much interest evoked evident size gap between 1 and 5 mm diameters of nodule sizes, explained by Menard (1964) as a result of different techniques of study. In the cited paper the maximum size of micronodule was established at 1 mm, with a clause that this limit was arbitrarily chosen. Similar extremal value (1—2 mm) was also adopted in Russian terminology (1973).

MODE OF OCCURRENCE

The investigated micronodules of Mn-, Fe- and Ca- carbonate composition similarly to their macro- equivalents have been found in majority of cases in the variegated shales of Palaeogene age of Carpathian Flysch. As yet, they were reported from the Lowest Eocene of the Skole tectonic unit, cored in Szklary IG 1 bore-hole, south of Rzeszów (Wieser, 1969) and from Middle Eocene Hieroglyphic beds of Magura tectonic unit, outcroping near Łętownia village south of Cracow (Borysławski and Wieser, 1981). Lately, the presence of birnessite (Mn-oxyhydroxide) in the form of micronodules and pseudomorphs after rhodochrosite-like minerals in association with birnessite macronodules and Ca-rhodochrosite crystals was established in Turonian Godula variegated shales of Silesian tectonic unit (near Lanckorona, south of Cracow, Geroch and Wieser, in press). Single rhomboedric Ca-rhodochrosite crystals were also found in similar variegated shales of Turonian age in External Silesian tectonic unit, cored in Łodygowice IG 1 bore-hole near Żywiec (Geroch and Nowak, 1980, p. 359; Geroch and Wieser in press). Synchronic position and analogous host sediments to the mentioned Ca-rhodochrosite crystals occurrences reveals a horizon of "dolomite" crystals distinguished by Czernikowski (1949, p. 180) in Silesian tectonic unit from vicinity of Węglówka, near Sanok.

In all indicated localities the host rock for manganiferous micronodules represented clayey to marly shales with different, rather small or scarse admixtures of quartz and rarer feldspar silt. Their colours range from brown-red to gray-green and from brick-red to red-brown, depending from oxidation state or manganese content, respectively. The dominating clay mineral kind varies from illite to mixed-layered montmorillonite/illite and montmorillonite, sometimes in association of a zeolite, namely — clinoptilolite.

The last mentioned assemblage of montmorillonite+mixed-layered illite/montmorillonite+clinoptilolite characterizes Lower Eocene brick-red to red-brown claystones cored in Szklary IG 1 bore-hole. Unusually fine, pelitic to subcolloidal and colloidal, granulation of bulk mass indicating slow-rate sedimentation, numerous Radiolaria casts (built by clinoptilolite), phosphate fish teeth and scales, and high MnO content (equaling 0.63 per cent at 179.35 m depth) allow to imply eupelagic character of this partly volcanogenic sediment. Towards top of claystone layer steadily rises and oscillates the calcium carbonate content (in the form of dolomite, calcite and Mg-calcite) of the rock not without influence on the chemistry of micronodules, ranging from rhodochrosite to Fe-rhodochrosite and oligonite+ankerite. The micronodules are regularly dispersed in the sediment, constituting only 0.05 to 0.1 per cent of total weight.

The second investigated micronodule occurrence in Middle Eocene Hieroglyphic beds, near Łętownia, showing Ca-rhodochrosite to manganocalcite composition, is included in a different lithotype. Composed of clayey and a little dolomitic siltstones to silty claystones they must be reckoned among sediments of turbidite-laminite origin. Green-blue-gray to ash-gray coloured they abound in quartz, soda-rich feldspar, chloritized biotite, chlorite rarer glauconite and coalified plant detrite, constituting silty fractions, as well as in illite, chlorite ±dolomite and calcite, concentrated in clayey fractions. The micronodules are irregularly dispersed in amounts comparable o the formerly reported, averaging 0.04—0.05 per cent of total rock weight.

PHYSIOGRAPHY AND CHEMISTRY

Methods. Samples of carbonate micronodules separated from disintegrated rock through ellutriation and heavy liquid selection were examined using optical and scanning microscopic, X-ray diffractometric, infra-red spectrophotometric, classical chemical, emission spectrographic and mass-spectrometric techniques.

Morphology and structure. The micronodules from Szklary and Łętownia localities differ radically in shape and in internal structure, accordingly with their chemical composition.

Three morphological varieties might be easily discerned in Szklary micronodule occurrence. First, nearly isometric variety (sample no. 48) from marly green-blue-gray to yellow-gray claystone usually ranges in size between 0.1—0.2 mm and is undoubtedly polycrystalline. This is easily detectable from their external surface, remembering sculpture characteristic for pyrites with framboidal structure (Pl. I. phot. 5 and 6). The internal irregularly granular and radial structure (Pl. II, phot. 5 and 6) is accentuated by deformed and diverging "optic crosses", as well as sectoral extinction, appearing in doubly polarized light images (under crossed nicols). Refractive index measurements revealed, moreover, zonary structure caused by ankerite overgrowth upon oligonite core. This phenomenon explains double peaks in the X-ray diffraction patterns (see Table 1). The reflection intensities of oligonite crystal lattices are nearly two times stronger than those of ankerite.

The second, barrel-shaped or ovaloidal variety derived from a little older brick-red claystone (sample no. 49, taken from 178 m depth in Szklary IG 1 bore-hole) is homogeneous, composed of Fe-rhodochrosite. The micronodules are a little larger (0.16—0.34 mm) and elongated (elongation ratio = 4:3—2:1). Provided with relatively a little smoother surface they exhibit terminal faces of unit rhombohedron $\{10\bar{1}1\}$ (see Pl. I, phot. 1, 2 and Pl. II, phot. 2). A small portion of the micronodules demonstrates contours with the concave angle due to epitaxial overgrowing and/or penetration twinning (Pl. I, phot. 1). Internal structure, judging from doubly-polarized light images (Pl. II, phot. 2) is more regularly radial than in the preceding variety. This is also visible from the fan-like distribution of fragmentary rhombohedric, originally etched figures resulting from framboidal-type structure (Pl. II, phot. 1). Rarely, appear micronodule subindividuals with two concave angles (e.g. with angle between long axes amounting 72°), in contour resembling "staurolite crosses", further those with three or more subindividuals.

The third, spindle-shaped variety (sample no. 51) from underlying red-brown claystone is also homogeneous, composed of rhodochrosite. It forms much more elongated (elong. ratio = 3:1—4:1) and insignificantly smaller (0.25—0.30 mm in length) grains. Their surfaces ofen display traces of a steep rhombohedron $\{40\bar{4}1\}$ faces in combination with an unit rhombohedron $\{10\bar{1}1\}$ terminal faces (Pl. I, phot. 3, 4). Epitaxial overgrowths with transitions to penetration twins examples (Pl. II, phot. 3.4) persist here much more frequently and the angles contained between long axes (*c*) are here distinctly variable and seldom repeated (in frequency order: 46°, 28°, 20°, 34°, 55°, 54° and 83°). The internal structure based on radiating arrangement of domains rests unchanged, assuming from the sectoral interference figures (extinction in opposite sectors) in doubly polarized light (Pl. II, phot. 4).

The Ca-rhodochrosite or manganocalcite micronodules from Łętownia occurrence (sample 8) distinguish their spherical shape of single globules and of globules joining in groups of coalesced spheres. These external features approach them conspicuously to normal (esp. calcite) macroconcretions. The internal structure of particular globule, ranging from 0.2 to 0.8 mm in size, corresponds to radial structure of oolites and similar sphaerocrysts or spherulites, but shows signs of recrystallization in the so-called granosphaerites. This is well visualized by deformation and lose of sharpness of the "optical crosses". The most common examples of such kind of micronodules are illustrated by micrographs of Plate III.

Crystallophysical data. X-ray diffractometric studies allow quick identification, including approximate determination of solid-solution crystal composition in binary or nearly binary systems. Much important in this evaluation seem d-spacings and especially *a* and *c* cell parameters and their ratio. Less suitable and credible, though more quickly obtainable and applicable to the smallest sample particles remain refractive index measurements (Wieser, 1952). They are listed with $d_{10.4}$ spacings and cell parameters in Table 1.

Comparing $d_{10.4}$ spacings, cell parameters, c/a ratios and refractive indices (n_ω) of oligonite (sample no. 48) with those for pure rhodochrosite and siderite one can deduce the rhodochrosite molecule content. It varies between 13 and 29 per cent, corresponding to Mn-siderites (5—25% $MnCO_3$) and to oligonites (25—75% $MnCO_3$). It is hard to say about the nature of other coexisting (overgrowing) mineral of the sample 48 without calculations basing on chemical analysis of the whole sample. The values for c/a and *c* parameter indicate the relationship with dolomite-ankerite crystal lattice ($a_{hex} = 4.810 \pm 0.002 - 4.819$, $c_{hex} = 16.02 \pm 0.001 - 16.10$ Å, $c/a = 3.330 - 3.341$, resp., after Howie and Broadhurst, 1958) and differ from that of kutnahorite ($a_{hex} = 4.8797$, $c_{hex} = 16.367$ Å, $c/a = 3.3541$ after Graf, 1961, p. 1285).

Table 1

D-spacings, cell parameters and refractive indices of examined micronodule and pure carbonate minerals

Sample no.	Carbonate mineral	$d_{10.4}$	a_{hex}*	c_{hex}*	c/a	n_ω
48	Oligonite	2.7979	4.701	15.405	3.277	1.858 (max.)
	Ankerite	2.8657	4.760	15.947	3.350	1.751—1.783
49	Fe-rhodochrosite	2.8562	4.789	15.761	3.291	1.819 (av.)
51	Rhodochrosite	2.8517	4.782	15.747	3.293	1.813 (av.)
8	Ca-rhodochrosite — manganocalcite	2.8935	4.824	16.045	3.326	1.756—1.792
—	Calcite	3.0359	4.990	17.061	3.419	1.658
—	Rhodochrosite	2.8440	4.777	15.664	3.279	1.816
—	Siderite	2.7912	4.686	15.297	3.264	1.875

* Cell parameters were established taking into account d-spacings of ten reflections. The data for pure carbonates are cited after Deer et al. (1962, p. 272) and Graf (1961, p. 1285).

These values suggest also adherence to manganocalcites (25—75% $MnCO_3$) but the chemical analytic data exclude such a supposition.

The d-spacings of other tabulated micronodule carbonate minerals are more reliable in calculations owing to more homogeneous structure of solid-solution (isomorphous mixture)-type, as was proved by chemical analyses. Namely, tabulated and non-tabulated data for Fe-rhodochrosite (sample no. 49 and 5) yielded siderite molecule contents ranging from 26 to 6 per cent, therefore, included between the limits proposed for Fe-rhodochrosite (75—95% $MnCO_3$). The corresponding interval for sample no. 51 amounted 23—0 per cent.

Among calciferous rhodochrosites and manganocalcites from Łętownia (sample no. a.o. 8) rhodochrosite molecule content basing on X-ray data and their derivatives oscillated between 78 and 67 per cent. The refractive index measurements disclosed larger interval, comprised between 84 and 60 per cent of $MnCO_3$ molecule. The chemical analysis for sample no. 8 only revealed well comparable results (71.6 mol. per cent $MnCO_3$) with those obtained from X-ray data (74, 78, 73, 67, with average = = 73 per cent).

Several specimens of micro-, as well as macronodules (see e.g., Gucwa and Wieser, 1978) of manganocalcite and Ca-rhodochrosite oscillated widely in Mn content, what implies the mutual substitution of Mn and Ca in the series calcite-rhodochrosite.

Practical application of infra-red spectroscopy to carbonate mineralogy increases continuously from year to year. Many writers pointed out that the carbonate minerals offer a possibility of qualitative identification and even semi-quantitative determination of some carbonate mineral mixtures (mechanical) and solid solutions. This

is well expressed in the example of rhodochrosite-siderite solid-solution system. Demonstrated in Fig. 1 infra-red spectra of two pure siderite samples (micronodules) and of examined oligonite (48) and Ferhodochrosite (49) disclose gradual shift of absorption bands from 728 cm^{-1} (49) to ca. 730 (48) and 738 cm^{-1} (siderites), following changes in the chemical composition. This is best marked for the mentioned double degenerate planar bending ($\nu_4, \Delta = 11.2$ cm^{-1} after Adler and Kerr, 1963) and much worse for out-of-plane bending (ν_2) and doubly degenerate asymmetric stretching (ν_3, $\Delta = 2.0$ and 0.7 cm^{-1}, resp.). In the range of ν_4 band ascribed to

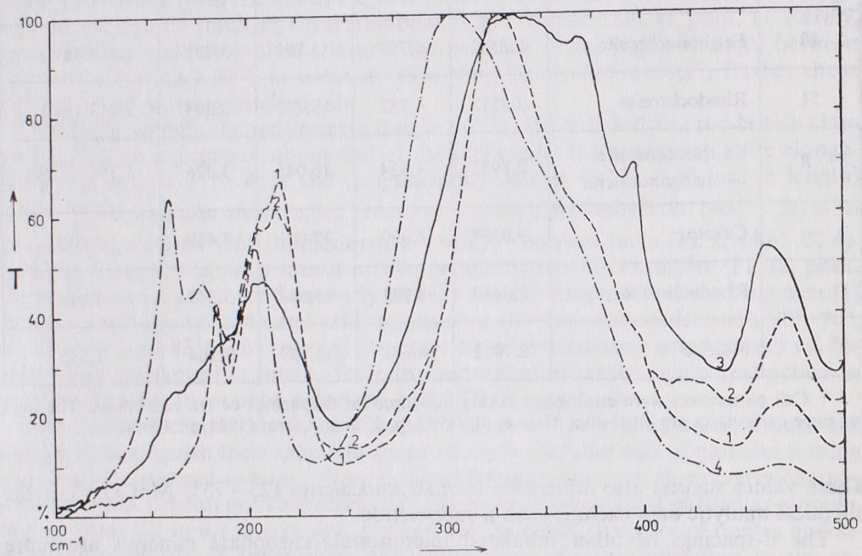

Fig. 1. Infra-red absorption spectra of the micronodules of Fe-rhodochrosite (*4*) and oligonite-ankerite (*3*) from Szklary in comparison with spectra of siderite micronodules from Dogger of Flysch Carpathians fore-land in frequency (ν) interval of 100—500 cm^{-1}. T = transmittancy

oligonite no additional maxima were observed. Instead, there is a small broadening, the result of ankerite admixture. The infra-red spectra in numerically small wave number interval of 100—500 cm^{-1} (Fig. 2) show much greater differences in curve tracks, interpretation of which is enigmatic and needs further studies.

Chemical data. Chemical analytic determinations were performed on all distinguished varieties of the carbonate micronodules. They provided additional informations regarding total, average chemical composition. The results of analyses executed using classical analytic methods, including spectrophotometric techniques are demonstrated in Table 2.

Moreover, the samples 48 and 49 were semi-quantitatively examined by H. Grabowski for the trace element contents with the aid of emission-spectrographic methods. The amounts of up to 2000 ppm Sr, 100 ppm Cu were determined in both samples, while Pb and Zn were present only in the sample no. 48 in amounts under 10 ppm. The elements Ba, V, U, Mo, Ni, Co occur in traces or are not detectable.

Besides substantial enrichment in Sr (probably in the form of admixed strontium mineral), and less expressed in Cu, striking is the far-reaching depletion in other metals, partly due to limited crystal lattice tolerance for ionic substitution in rhodochrosites and related carbonate minerals.

One of the most important generalizations emerging from environmental studies of micronodule nucleation and growth is the statement, that these processes took place in an approximately closed environment, that is, in equilibrium with surrounding,

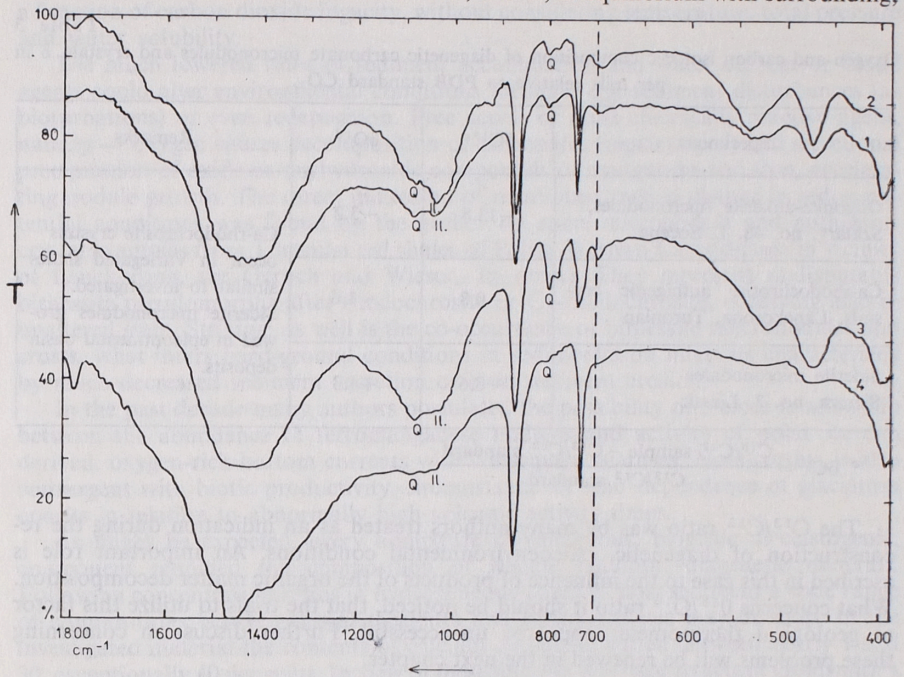

Fig. 2. Infra-red absorption spectra for the same specimens of micronodules as in Fig. 1, but in the frequency interval of 400—1800 cm^{-1}.

Table 2

Chemical analyses of carbonate micronodules in weight (oxides) and molecular (carbonates) per cents

Sample no.	Mineral variety	MnO	FeO	MgO	CaO	$MnCO_3$	$FeCO_3$	$MgCO_3$	$CaCO_3$
48	Oligonite +ankerite	22.80	28.53	3.65	5.51	35.5	43.7	10.0	10.8
49	Fe-rhodochrosite	56.78	3.31	0.39	0.37	92.8	5.3	1.1	0.8
51	Rhodochrosite	58.84	1.41	0.67	0.46	94.9	2.3	1.9	0.9
8	Manganocalcite*	44.15	0.63	0.56	14.10	69.4	1.0	1.6	28.0

* Analyst: J. Tarkowski; remaining analyses performed by author.

especially hydrological system. In this relation, carbon and oxygen isotopic compositions become helpful factors for further considerations. Mass-spectrometric determinations comprised one (no. 48) of the investigated samples and, for comparison reasons, two other carbonate, diagenetic mineral instances, as well. The data are presented below in Table 3.

Table 3

Oxygen and carbon isotopic composition of diagenetic carbonate micronodules and crystals. δ in per mils relative to PDB standard CO_2.

Specimens	δC^{13}*	δO^{18}	Remarks
Oligonite-ankerite micronodules, Szklary, no. 48. L. Eocene	−13.8	−3.2	Ca-rhodochrosite crystals occur in Variegated shales similar to investigated. Siderite micronodules growed in epicontinental basin deposits.
Ca-rhodochrosite authigenic crystals, Lanckorona, Turonian	−0.8	−1.6	
Siderite micronodules Siercza, no. 2, Liassic	−8.6	+1.3	

$$* \quad \delta C^{13} = \frac{C^{13}/C^{12} \text{ sample} - C^{13}/C^{12} \text{ standard}}{C^{13}/C^{12} \text{ standard}}$$

The C^{13}/C^{12} ratio was by many authors treated as an indication during the reconstruction of diagenetic, paleoenvironmental conditions. An important role is ascribed in this case to the influence of products of the organic matter decomposition. What concerns O^{18}/O^{16} ratio it should be noticed, that the trials to utilize this factor as geological thermometer appeared unsuccessful. Further discussion concerning these problems will be renewed in the next chapter.

DISCUSSION AND CONCLUSIONS

The origin of manganese micronodules has not received as much attention as of the corresponding macronodules. So far as present knowledge extends, there is no reason to believe that in comparison with the micronodules their proto-macronodule equivalents might have a special origin. Showing no remarkable differences in the mineralogical constitution, the structural peculiarity of micronodules in the form of preponderance of spherulite-type structures is an obvious phenomenon, when they are treated as a nucleation stage of macronodules. These "in statu nascendi" nodules growed up in a closed environment of sediments enriched in partly or completely hydrolyzed volcanic glass (like: smectitized, zeolitized + Mn—Fe oxyhydroxides).

High productivity of organic, specially microplanktonic, matter in volcanic epochs, after quick burial, favoured its accumulation in sediments. All writers agree, that the decaying organic matter stimulates mobilization (esp. of Mn a.o. metal ions and acid radicals) and migration of hydrolysates by pore waters. This is not a question of accident; as was proved through many examples of a strict coexistence of organic relicts and micronodules (e.g. Greenslate, 1974; Thiel, 1978 a.o.).

Changes in the carbon dioxide partial pressure and in the pH and E_h gradient between surficial and underlying deposits may create diffusion potential promoting

ascenzional movement toward bottom surface. When surficial conditions became neutral or reductional and the sediment is adequately rich in metal-hydrolysates then begins the rhodochrosite precipitation. Huebner (1969) argued experimentally that siderite against rhodochrosite is less stable at higher oxygen fugacity, what radically enlarges stability field of rhodochrosite. Stability field of rhodochrosite is also a function of carbon dioxide fugacity, without considering temperature, total pressure and water solubility.

The much lowered rates of sediment accumulation and water current or biotic agents could alter environmental conditions through, e.g. sediment disturbances (as bioturbations) or even redeposition. Free access of most chemically reactive agent, namely — oxygen causes decomposition of carbonates (replacement) and secretional precipitation of oxide or oxyhydroxide compounds of manganese and iron, accelerating nodule growth. The direct indication of mentioned radical change in redox potential conditions was found by the author on some micronodule and authigenic crystal examples from Turonian red shales of Polish Western Carpathians (in vicinity of Lanckorona, see Geroch and Wieser, in press). They represent undisputable birnessite pseudomorphs after rhodochrosite or Ca-rhodochrosite, occurring also in unaltered state. Striking, as well is the co-occurrence of birnessite macronodules and crusts, what infers hard-ground conditions in sedimentation intervals characterized by much decreased sediment accretion or even sediment erosion.

In the past decade many authors postulated the possibility of a close relationship between the abundance of ferromanganese nodules and activity of polar ice cap derived, oxygen-rich bottom currents with consequent hiatuses. Noteworthy, is also convergent with biotic productivity circumstance of the dependence of glaciation epochs in relation to abnormally high volcanic activity times.

As might be expected, every admixture of calcareous, biogenic or clastogenic, component modified the composition of nodule building, diagenetic minerals. Following concentration ratios in hydrogeneous phase of host sediment a wide range of compositions between manganocalcites and rhodochrosites may develop. In the investigated material the contents of calcium carbonate varied between nearly 1 and 30, exceptionally 40 per cents. In view of these findings it is hard to accept Goldsmith's and Graf's (1957) conclusion implying the existence under 550°C, of a solubility gap in the interval 20—50 per cent of $CaCO_3$ in the $CaCO_3$—$MnCO_3$ system. Lynn and Bonatti (1965) announced the occurrence of indurated masses of Mn, Ca-carbonate mineral with variable composition (Mn ranging from 50 to 80 per cent) in a core from a bore-hole piercing Pacific deposits. Undoubtedly, the presence of additional ions (like Fe, Mg) facilitates ionic substitution (mutual diadochy), expressed in the enlargement of stability field in diagenetic régime. This stays in agreement with Huebner's (1969) conclusion emphasizing, that carbonates chemically approximating the rhodochrosite composition are less common than manganiferous Ca-, Mg- and Fe-carbonates.

Under CCD (carbonate compensation depth) carbon dioxide source in the form of carbonate detrite must be excluded from consideration and replaced by connected with organic matter decay. As a consequence it follows, that a far reaching limitation of carbonate composition, mainly to siderite-rhodochrosite solid-solution system must be induced. The mentioned system, judging only from analytic data of macronodules is deprived of a solubility gap and rhodochrosite-rich members seem to indicate more deep bathymetric conditions. Such a supposition may be deduced in the instance of Szklary micronodule occurrence, envisaging paleogeographical situation. Provenance from deepest red clay deposits, filling newly formed Palaeocene-Eocene trench, distinguishes extremely low iron content in rhodochrosite micronodules. Towards the top, in the some thirty metres accounting red clay bed (Wieser, 1969),

increases the siderite molecule content to ca. 5 per cent. At last, after the change of rock colouring in olive- to blue-gray (ca. sixty m above trench bottom), simultaneously with calcareous detrite admixture, appear the oligonite+ankerite micronodules, connected with amaller depths, just above CCD. The addition of calcareous detrite contributed to the lowering of δC^{13} value (to −13.8 per mils, see Table 3). It has long been recognized that the value of C^{13}/C^{12} ratios of siderite is an useful instrument in interpretation of ancient sedimentary environment. Weber et al. (1964) arbitrarily set $\delta C^{13} = -2.5$ per mil as a limit between fresh-water and brackish marine siderite nodules and plates. A little later Hodgson (1966) systematically investigated carbon and oxygen isotopic ratios in diagenetic carbonates from marine sediments, acquiring much conclusive results. The isotopic compositions of diagenetic carbonates including nodules and lenses with spherulitic texture from marine Tertiary to Cambrian horizons showed, that they are strikingly different against measured in normal marine limestones and above mentioned siderites. The lightest carbonates with δC^{13} falling to −54 per mil represented Jurassic rhodochrosite concretions and lenses with spherulitic texture, and the values for other diagenetic Mn-carbonates amounted: −6.9, −17.2, −17.7, −39.4 and −49.7. For comparison, those for Fe-carbonates oscillated between −19.7 and −33.3 and for Ca-carbonates — between+2.4 and −29.5. Taking into account measurement results recorded by Hodgson (op. cit., fig. 2) after literature data for marine (+4 to −2) and fresh-water limestones (−2 to −13) against those for organic matter and bitums from marine sediments (−19 to −30), attractive becomes assumption, that the carbon for limestones was more or less modified in isotopic composition through contamination by atmospheric carbon dioxide ($\delta C^{13} = -7$ to −10) or oxidation products of organic matter. In the last case of marine organic matter (more or less bituminized) abundant availability of light carbon dioxide should be attributed to isotopic fractionation process in the form of enzymic decarboxylation of organic compounds (with Bacteria participation) of marine ±land plants, at low temperatures. The gaseous hydrocarbons (e.g. methane) have even higher C^{12} content than liquid (e.g. petroleum). This same writer remarks also, after a study of oxygen isotopic composition of coexisting calcite and rhodochrosite that, whereas the latter has retained its isotopic composition from the period of precipitation, the calcite has undergone equilibration during diagenesis.

This and former statements explain together with mentioned eventual influence of calcareous debris contamination a striking isotopic peculiarity of ferromanganese deep-sea macro- and micronodules, which may be employed as bathymetric indicator after further studies. In this context remarkable is Hodgson's opinion inferring: "there is no reason to suppose that extremely light carbon is only to be found in rhodochrosite".

Another potential criterion useful in a palaeoenvironmental analysis in the form of macro- and microelement spectra seems to be less promising in the case of micronodules. The deciding reason is much limited crystal lattice tolerance for substitution phenomena, already observed in carbonate macronodules (e.g. Gucwa, Wieser, 1978 and Muszyński et al., 1978), as well as in the investigated samples of micronodules. However, noteworthy are differences in macro- and microelements spectra between common (oxyhydroxide or oxide) ferromanganese macronodules and micronodules of actual oceans deposits. Known as "metal scavengers", owing to richness in various metals, the macronodules basing on Addy's (1978) conclusions show, moreover, higher Mn/Fe ratio and Ni, Co and Cu concentrations than coexisting micronodules, especially small ones. Only in the micronodules from siliceous oozes Ni and Cu contents are as high as in the micronodules. These relations can be interpreted, as follows: the micronodules or proto-macronodules in clayey sediments were primarily of carbonate composition and only in the following stages of growth they were partly or

totally replaced by Mn—Fe oxyhydroxides and oxides, which could also grow as primary minerals. This way micronodule may become enriched in manganese and trace elements. Present study supports the conception, that the micronodules just from the start of growth (nucleation stage) were ferromanganese carbonates (rhodochrosites to oligonites). This is also justified, taking into account small water solubility and greater stability with rising oxygen fugacity of rhodochrosite against siderite and other carbonates.

When the origin of micronodules can be without clause acknowledged as diagenetic, that of macronodules might have been partly diagenetic (precipitation from pore waters) and partly hydrogeneous (s. stricto, by precipitation from sea-water). If burial by subsequent sediments will not cease growing, the nodules may incorporate a plenty of chiefly hydrogeneous elements, like manganese, nickel, cobalt or copper. Radiochemical studies conducted by Ku and Broecker (1969) revealed that the accretion rates for nodules amounted only 1 to 6 mm/10^6 years, values comparable to the slowest sedimentation rates of pelagic-type sediments. Chester and Hughes (1969) estimated that, between 80—90 per cent of total Mn has a hydrogeneous origin and from this amount as much as 85 per cent of the Mn in pelagic sediments occurs in the micronodules. The equivalent values for Co and Ni are, as follows: 68 and 95 or 51——89 and 40—72 per cent., respectively. Strong correlation between Mn and Cu, Ni, Co, Zn suggests after Piper et al. (1979) that these metals may be bound in a single phase, possibly in micronodules. The greater abundance of nodules in the Pacific compared to the Atlantic Ocean, excluding volcanic activity participation, probably reflects lower sediment accretion rate in the former ocean. The post-burial dissolution of the nodules might reduce their representation in older sediments of stratigraphic column.

Similar opinions were expressed in the last paper written by Marchig and Grundlach (1979) in the words: "the population of micronodules decreases with depth in the sediment within first 35 cm. Only 5 per cent of the amount of micronodules at the sediment surface was found at 35 cm. In addition the Mn, Ni, Cu and Zn contents of the micronodules decrease with depth and the Fe content increases. These observations indicate partial dissolution and remobilization of micronodules buried under the sediment-water interface boundary layer (as Soren et al., 1978, defined it). Manganese, as the more soluble component and the ions incorporated in or adsorbed on manganese hydroxide are preferentially remobilized; Fe, Si, and Al being less soluble than Mn become more concentrated in remaining micronodules". It must be remembered, however, that these considerations concern more oxidized environment and in the here presented case almost no signs of dissolution or remobilization of carbonate micronodule substance might be noted.

FINAL REMARKS

The carbonate and other manganiferous micronodules are extremely rare in sediments of former oceans occurring now on land surface. It is possible that it is a question of lack of rationally directed researches, which should be concentrated on pelagic-type, e.g. geosynclinal sediments. During micropaleontological preparatory works advantageous material is sometimes available without further evaluations and investigations.

The composition of the micronodules allows the reconstruction of paleoenvironmental conditions of diagenesis. Among carbonate micronodules, rhodochrosite and rhodochrosite-siderite solid-solution system minerals are most stable in non-calcareous, organic matter-rich sediments. The carbon dioxide derived from enzymic

decarboxylation of organic matter has specific isotopic composition (Hodgson, 1966), which is also unalterable. This can not be said in the case of sediments originating above *CCD* (carbonate compensation depth), contaminated by calcareous debris. Probably this will be utilized as a bathymetric indicator.

The morphological and structural features of manganese and ferromanganese carbonate micronodules consequently vary (e.g. the habit from isometric do spindle-shaped) in iron content, which decreases with increasing depth. Rhodochrosite probably characterizes the deepest sediments, that is diagenetic conditions with highest CO_2 fugacities. It is also more stable than siderite at higher oxygen fugacities and temperatures (Huebner, 1969). Peculiar spherical habit exhibit manganocalcite and Ca-rhodochrosite micronodules formed in not typically eupelagic sediments above *CCD*, contaminated with calcareous detrite.

The depleted trace element content of examined micronodules may be interpreted as a consequence of low crystal lattice tolerance of rhodochrosite and related carbonates for ionic substitution. Besides, remarkable is the paucity of dissolution phenomena and lack of signs of Mn and Fe remobilization, typical for oxyhydroxide micronodules, usually enriched in trace elements.

Acknowledgments: The author is grateful to following persons for performance of the cited determinations, like: carbon and oxygen isotopic composition to dr Jerzy Grabczak, chemical analyses of Ca, Mn-carbonates to mgr Jan Tarkowski, infra-red spectrophotograms to ing. Czesława Paluszkiewicz and spectrographic analyses of trace elements to mgr Henryk Grabowski.

REFERENCES

ADDY S. K., 1978: Distribution of Fe, Mn, Cu, Ni and Co in coexisting manganese nodules and micronodules. *Mar. Geol.* 28, no. 1/2, M9—M17.

ADLER H. H., KERR P. F., 1963: Infrared absorption trends for anhydrous normal carbonates. *Amer. Miner.* 48, 124—137.

BORYSŁAWSKI A., WIESER T., 1981: Mikrokonkrecje węglanowe w warstwach hieroglifowych podjednostki raczańskiej (płaszczowina magurska). *Kwart. Geol.* 25, 821—822.

CHESTER R., HUGHES M. J., 1969: The trace element geochemistry of a North Pacific pelagic clay core. Deep-Sea Research 16, 639—654.

CZERNIKOWSKI J., 1949: Otwornice serii fliszowej facjesu śląskiego na pograniczu kredy górnej i dolnej. *Nafta* 5, no. 7—8, 177—180.

DEER W. A., HOWIE R. A., ZUSSMAN J., 1962: Rock-forming Minerals, vol. 5, Non-Silicates, Longmans, London.

EL WAKEEL S. K., RILEY J .P., 1961: Chemical and mineralogical studies of fossil red clays from Timor. Geoch. et Cosmoch. Acta 24, 260—265. [Geological Dictionary] Геологический Словар, Изд. Недра, Москва, 1973.

GEROCH S., NOWAK W., 1980: Stratygrafia fliszu w odwiercie Łodygowice IG-1 w Karpatach. *Rocz. Pol. Tow. Geol.* 50, no. 3/4, 341—390.

GLASBY G. P., 1978: Deep-sea manganese nodules in the stratigraphic record: evidence from DSDP cores. *Mar. Geol.* 28, 51—64.

GOLDSMITH J. R., GRAF D. L., 1957: The system CaO—MnO—CO_2: Solid-solution and decomposition relations. *Geoch. et Cosmoch. Acta* 11, 310—334.

GRAF D. L., 1961: Crystallographic tables for the rhombohedral carbonates. *Amer. Miner.* 46, 1283—1316.

GREENSLATE J., 1974: Manganese and biotic debris associations in some deep-sea sediments. Science 186, 529—531.

GUCWA I., WIESER T., 1978: Ferromanganese nodules in the Western Carpathian Flysch deposits of Poland. *Rocz. Pol. Tow. Geol.* 48, 147—182.

HODGSON W. A., 1966: Carbon and oxygen isotope ratios in diagenetic carbonates from marine sediments. *Geoch. et Cosmoch. Acta* 30, 1223—1233.

HOWIE R. A., BROADHURST F. M., 1958: X-ray data for dolomite and ankerite. *Amer. Miner.* 43, 1210—1214.

HUEBNER J. S., 1969: Stability relations of rhodochrosite in the system manganese-carbon-oxygen. *Amer. Miner.* 54, 457—481.

JENKYNS H. C., 1977: Fossil nodules. In G. P. Glasby (Editor), Marine manganese deposits, 87—108, Elsevier, Amsterdam.

[KOSSOVSKAYA A. G., DRITZ W. A.] Коссовская А. Г., Дриц В. А., 1978: Минералого-петрографическое описание пород скважины 345. Результаты глубоководного бурения в Атлантическом океане в 38-м рейсе „Гломар Челленджера". Литол. и петр. 43-51, Наука, Москва, 1979.

KU T. L., BROECKER W. S., 1969: Radiochemical studies on manganese nodules of deep-sea origin. *Deep-sea Res.* 16, 625—637.

LYNN D. C., BONATTI E., 1965: Mobility of manganese in diagenesis of deep-sea sediment. *Mar. Geol.* 3, 457—474.

MARCHIG V., GUNDLACH H., 1979: Changes in chemical composition of some Pacific manganese nodules during their growth. In J. L. Bischoff and D. Z. Piper (Editors): Marine Geology and Oceanography of the Pacific Manganese Nodule Province, 729—746, Plenum Press, New York, London.

MENARD H. W., 1964: Marine Geology of the Pacific, McGraw-Hill, New York.

MUSZYŃSKI M. J., PAJCHEL J., SALAMON W., 1978: Concretionary iron and manganese carbonates in Eocene shales of the environs of Dynów near Przemyśl (Flysch Carpathians). *Mineral. Polon.* 9, no 1, 111—120.

PIPER D. Z., LEONG K., CANNON W. P., 1979: Manganese nodule and surface sediment composition: Domes sites A, B, and C. In J. L. Bischoff and D. Z. Piper (Editors): Marine Geology and Oceanography of the Pacific Manganese Nodule Province, 437—473, Plenum Press, New York, London.

STACKELBERG U. v., (1979): Sedimentation, hiatuses and development of manganese nodules: Valdivia site VA-13/2, Northern Central Pacific. In J. L. Bischoff and D. Z. Piper (Editors): Marine Geology and Oceanography of the Pacific Manganese Nodule Province, 559—586, Plenum Press, New York, London.

THIEL H., 1978: The faunal environment of manganese nodules and aspects of deep-sea time scales. In: Environmental biochemistry and geomicrobiology 3, *Ann Arbor Sci.*, 887—896.

[VARENTSOV I. M., DRITZ W. A.,] Варенцов И. М., Дриц В. А., 1978: Литолого-минералогическое изучение образований осадочного чехла по скважине 350. „Результати глубоководного бурения в Атлантическом океане в 38-м рейсе „Гломар Челленджера". Литология и петрография 83-101, Наука, Москва, 1979.

WEBER J. N., WILLIAMS E. G., KEITH M. L., 1964: Paleoenvironmental significance of carbon isotopic composition of siderite nodules in some shales of Pennsylvanian age. *Jour. Sed. Petrol.* 34, 814—818.

WIESER T., 1952: Simplified immersion method for determination of the refractive indices of minerals and liquids by means of a polarization microscope. *Rocz. Pol. Tow. Geol.* 22, 319—338.

WIESER T., 1969: Clinoptilolite from the Lower Eocene Variegated Shales of the External Flysch Carpathians. *Bull. Acad. Pol. Sci., Sér. Géol. et Géogr.* 17, 123—129.

Tadeusz WIESER

MANGANONOŚNE MIKROKONKRECJE WĘGLANOWE OSADÓW POLSKICH KARPAT FLISZOWYCH I ICH POWSTAWANIE

Streszczenie

Głębokomorskie, diagenetyczne mikrokonkrecje węglanowe występują w pelagicznych iłowcach najniższego eocenu skolskiej jednostki tektonicznej oraz w bardziej mulastych i nieco wapnistych, szarawych osadach środkowego eocenu (warstwy hieroglifowe) magurskiej jednostki tektonicznej fliszu karpackiego.

Węglany budujące mikrokonkrecje z największych głębokości znamionuje skład rodochrozytowy a mikrokonkrecje — pokrój wrzecionowaty. Na nieco mniejszych głębokościach powstawały mikrokonkrecje Fe-rodochrozytowe z beczułkowatym

pokrojem a najpłyciej, w pobliżu CCD — mikrokonkrecje oligonitowo-ankerytowe z izometrycznym pokrojem. Środkowoeoceńskie mikrokonkrecje manganokalcytowe do Ca-rodochrozytowych tworzyły się w osadach mniej typowo pelagicznych, powyżej CCD i wyróżniają się kulistym pokrojem (tzw. globule).

Mikrokonkrecje węglanowe są bogate w lekki izotop C^{12}, którego zawartość jest najwyższa i niezmienna w odmianach rodochrozytowych do oligonitowych.

Ubóstwo mikroelementów w badanych mikrokonkrecjach jest następstwem niskiej tolerancji sieci krystalicznej rodochrozytu i pokrewnych węglanów na substytucję jonową.

OBJAŚNIENIA FIGUR

Fig. 1. Widma absorpcyjne w poczerwieni mikrokonkrecji Fe-rodochrozytu (*4*) i oligonitu-ankerytu (*3*) ze Szklar w zestawieniu z widmami mikrokonkrecji syderytowych z doggeru przedpola Karpat fliszowych w przedziale częstości drgań (ν) 100—500 cm^{-1}. T = przepuszczalność (światła)

Fig. 2. Widma absorpcyjne w podczerwieni dla tych samych próbek mikrokonkrecji jak w fig. 1 lecz w przedziale częstości drgań 400—1800 cm^{-1}.

OBJAŚNIENIA FOTOGRAFII

Plansza I

Fot. 1. Obraz beczułkowatej mikrokonkrecji Fe-rodochrozytowej ze Szklar (dolny eocen) w elektronowym mikroskopie skaningowym, przedstawiający rzeźbę powierzchni właściwą dla budowy framboidalnej oraz jednostkowy romboedr jako terminalną postać prostą. Pow. ×100

Fot. 2. Ten sam rodzaj mikrokonkrecji widoczny w mikroskopie optycznym. Nikole równoległe. Pow. ×17

Fot. 3. Obraz wrzecionowatej mikrokonkrecji rodochrozytowej ze Szklar w elektronowym mikroskopie skaningowym ukazujący stromy romboedr {40$\bar{4}$1} jako postać prostą. Pow. ×180.

Fot. 4. Ten sam rodzaj mikrokonkrecji widoczny w mikroskopie optycznym, z przykładami bliźniaków penetracyjnych. Nikole równoległe. Pow. ×13

Fot. 5. Obraz oligonitowo-ankerytowej mikrokonkrecji ze Szklar w elektronowym mikroskopie skaningowym ujawniający pokrój izometryczny i powierzchnię podobną do związanej z budową framboidalną. Pow. ×310

Fot. 6. Ten sam rodzaj mikrokonkrecji widoczny w mikroskopie optycznym. Nikole równoległe. Pow. ×15

Plansza II

Fot. 1. Obraz kolankowego bliźniaka kontaktowego — beczułkowatej mikrokonkrecji Fe-rodochrozytowej ze Szklar w elektronowym mikroskopie skaningowym. Pow. ×65

Fot. 2. Beczułkowata mikrokonkrecja ujawniająca sektorowe wygaszanie światła wskutek wachlarzowatego sposobu wzrostu. Nikole skrzyżowane. Pow. ×32

Fot. 3. Obraz wrzecionowatej mikrokonkrecji z różnie zorientowanymi naroślami i/lub penetracyjnymi bliźniakami w elektronowym mikroskopie skaningowym. Pow. ×150

Fot. 4. Wrzecionowata mikrokonkrecja wykazująca sektorowe wygaszanie światła. Nikole skrzyżowane. Pow. ×55 i 86

Fot. 5. Równowymiarowa mikrokonkrecja oligonitowo-ankerytowa ujawniająca budowę prawie promienistą do rozbieżnej. Nikole skrzyżowane, pow. ×75

Fot. 6. Jak na fot. 5. Pow. ×120

Fot. 1. Obraz mikroskopowy pojedynczej kulistej i dwu przerosłych mikrokonkrecji Ca-rodochrozytowych lub manganokalcytowych z Łętowni (śr. eocen). Światło odbite. Pow. ×35

Fot. 2-4. Wielokrotne i nieregularnie przerosłe mikrokonkrecje Ca-rodochrozytowe lub manganokalcytowe na wzór kalcytowych makrokonkrecji, ukazujące lśniącą, gładką powierzchnię jak na fot. 1. Światło odbite. Pow. ×40 i 50 (fot. 4)

Fot. 5 i 6. Obrazy dla cienkich płytek powyższych mikrokonkrecji ukazujące budowę bezładnie promienistą do ziarnistej granosferytów. Światło przechodzące, nikole skrzyżowane, pow. ×87 i 72, odp.

Тадеуш ВИЗЭР

МАРГАНЦЕНОСНЫЕ КАРБОНАТНЫЕ МИКРОКОНКРЕЦИИ В ОТЛОЖЕНИЯХ ПОЛЬСКИХ ФЛИШЕВЫХ КАРПАТ И ИХ ОБРАЗОВАНИЕ

Резюме

Глубоководные диагенетические карбонатные микроконкреции присутствуют в пелагических аргиллитах низов зоцена скольской тектонической единицы, а также в более алевритистых и немного известковистых сероватых среднеэоценовых отложениях (иероглифовые слои) магурской тектонической единицы карпатского флиша.

Карбонаты, слагающие микроконкреции из самых больших глубин, отличаются родохрозитовым составом, а микроконкреции — веретенообразной формой. На немного меньших глубинах образовались Fe-родохрозитовые конкреции бочонковидной формы, а в более мелководной зоне, в близи CCD (глубины карбонатного уравновешивания) — олигонит-анкеритовые микроконкреции изометрической формы. Среднеэоценовые манганокальцитовые до Ca-родохрозитовые микроконкреции образовались в отложениях не совсем пелагического типа, выше CCD и отличаются шаровидной формой (так называемые глобули).

Карбонатные микроконкреции богатые легким изотопом C^{12}, содержание которого самое высокое и постоянное в родохрозитовых до олигонитовых разновидностях.

Бедность микроэлементов в изучаемых микроконкрециях является следствием небольшой толерантности кристаллической решетки родохрозита и родственных карбонатов на ионное замещение.

ОБЪЯСНЕНИЯ К ФИГУРАМ

Фиг. 1. Сопоставление ИК-спектров микроконкреций Fe-родохрозита (*4*) и олигонит-анкерита (*3*) из Шкляров со спектрами сидеритовых микроконкреций из доггера флишевых Карпат, диапазон частот колебаний (ν) 100—500 $см^{-1}$. T = просвечиваемость

Фиг. 2. ИК-спектры для тех же самых образцов микроконкреций что на фиг. 1, но в диапазоне частот колебаний 400—1800 $см^{-1}$

ОБЪЯСНЕНИЯ К ФОТОГРАФИЯМ

Таблица I

Фото 1. Электронно-микроскопическое изображение Fe-родохрозитовой микроконкреции из Шкляров (нижний зоцен), представляющее скульптурную поверхность, типичную для фрамбоидального строения, а также единичный ромбоэдр в качестве конечной простой формы. Увел. × 100

Фото 2. Этот же самый вид микроконкреции в оптическом микроскопе. Параллельные николи Увел. × 17

Фото 3. Электронно-микроскопическое изображение родохрозитовой микроконкреции из Шкляров, показывающее крутой ромбоэдр ($40\bar{4}1$) в качестве простой формы. Увел. × 180.

Фото 4. Этот же самый вид микроконкреции в оптическом микроскопе с примерами пенетративных двойников. Параллельные николи. Увел. × 13

Фото 5. Электронно-микроскопическое изображение олигонит-анкеритовой микроконкреции из Шкляров, обнаруживающее изометрический габитус и поверхность схожую с фрамбоидальным строением. Увел. × 310

Фото 6. Этот же самый вид микроконкреции в оптическом микроскопе. Параллельные николи. Увел. × 15

Таблица II

Фото 1. Электронно-микроскопическое изображение коленчатого контактного двойника бочонковидной Fe-родохрозитовой микроконкреции из Шкляров. Увел. × 65

Фото 2. Бочонковидная микроконкреция, обнаруживающая секторное погасание света вследствие веерообразного способа роста. Скрещенные николи. Увел. × 32

Фото 3. Электронно-микроскопическое изображение веретенообразной микроконкреции с различной ориентировкой наростов и (или) пенетративными двойниками. Увел. × 150

Фото 4. Веретенообразная микроконкреция, обнаруживающая секторное погасание света. Скрещенные николи. Увел. × 55 и × 86

Фото 5. Равноразмерная олигонит-анкеритовая микроконкреция, обнаруживающая почти радиально-лучистое до расходящегося строение. Скрещенные николи. Увел. × 75

Фото 6. То же самое что на фото 5. Увел. × 120

Таблица III

Фото 1. Микроскопическая картина одиночной шаровидной и двух срастающихся Ca-родохрозитовых или манганокальцитовых микроконкреций из Лэнтовни (средний зоцен). Отраженный свет. Увел. × 35

Фото 2—4. Многократные и нерегулярные срастания Ca-родохрозитовые или манганокальцитовые микроконкреции на подобие кальцитовых макроконкреций, обнаруживающие блестящую гладкую поверхность как на фото 1. Отраженный свет. Увел. × 40 и × 50 (фото 4)

Фото 5—6. Картина вышеуказанных микроконкреций в шлифах, обнаруживающая неупорядоченное радиально-лучистое строение до зернистого строения граносферитов. Проходящий свет. Скрещенные николи. Увел. × 87 и 72 соответственно

EXPLANATIONS OF PHOTOGRAPHS

Plate I

Phot. 1. Scanning electron micrograph of barrel-shaped Fe-rhodochrosite micronodule from Szklary (Lower Eocene) demonstrating surface sculpture peculiar for framboidal structure and a unit rhombohedron as terminal simple form. Magn. ×100

Phot. 2. The same kind of micronodules in optic microscope image. Parallel nicols. Magn. ×17

Phot. 3. Scanning electron micrograph of spindle-shaped rhodochrosite micronodule from Szklary showing a steep rhombohedron $\{40\bar{4}1\}$ simple form. Magn. ×180

Phot. 4. The same kind of micronodules in optic microscope image, with examples of penetration twins. Parallel nicols. Magn. ×13

Phot. 5. Scanning electron micrograph of oligonite-ankerite micronodule from Szklary exhibiting an isometric habit and surface similar to that connected with framboidal structure. Magn. ×310

Phot. 6. The same kind of micronodules in optic microscope image. Parallel nicols. Magn. ×15

Plate II

Phot. 1. Scanning electron micrograph of elbow-shaped contact twin of barrel-type Fe-rhodochrosite micronodule from Szklary. Magn. ×65

Phot. 2. Barrel-shaped micronodule exhibiting sectoral light extinction due to fan-like growth. Crossed nicols. Magn. ×32

Phot. 3. Scanning electron micrograph of spindle-shaped micronodule with differently oriented overgrowths and/or penetration twins. Magn. ×150

Phot. 4. Spindle-shaped micronodule showing sectoral light extinction. Crossed nicols. Magn. ×55 and 86

Phot. 5. Equidimensional oligonite-ankerite micronodule displaying nearly radial to divergent structure. Crossed nicols, Magn. ×75

Phot. 6. As in Phot. 5. Magn. ×120

Plate III

Phot. 1. Micrograph of a single spherical and two intergrown Ca-rhodochrosite or manganocalcite micronodules from Łętownia (Middle Eocene). Reflected light. Magn. ×35

Phot. 2—4. Multiple and irregularly intergrown Ca-rhodochrosite or manganocalcite micronodules resembling calcite macroconcretions and showing shining, smooth surface as in Phot. 1. Reflected light, Magn. ×40 and 50 (Phot. 4)

Phot. 5 and 6. Thin section images of above mentioned micronodules showing irregularly radial to almost granular structure of granosphaerites. Transmitted light, crossed nicols. Magn. ×87 and 72, resp.

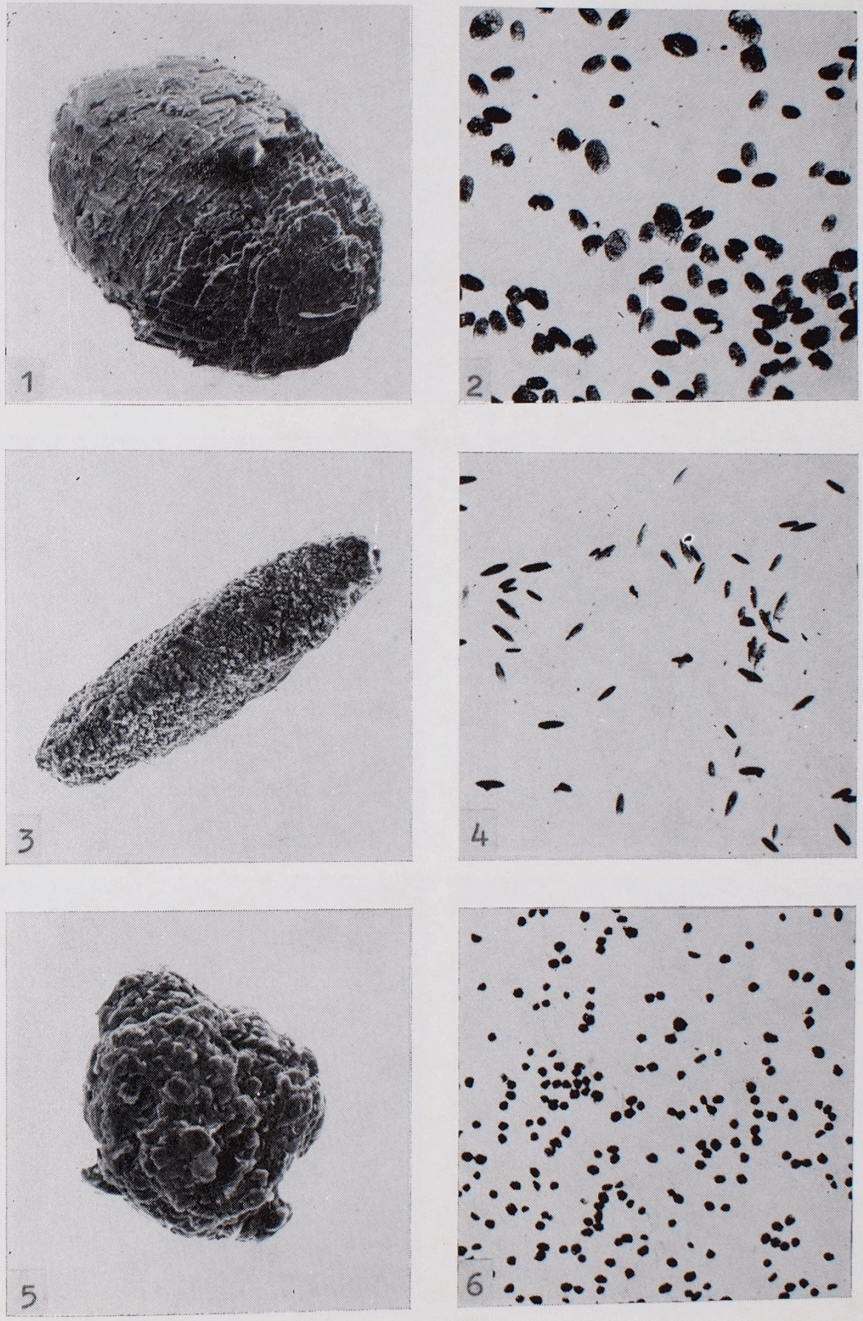

Tadeusz WIESER — Manganiferous carbonate micronodules of the Polish Carpathians Flysch deposits and their origin

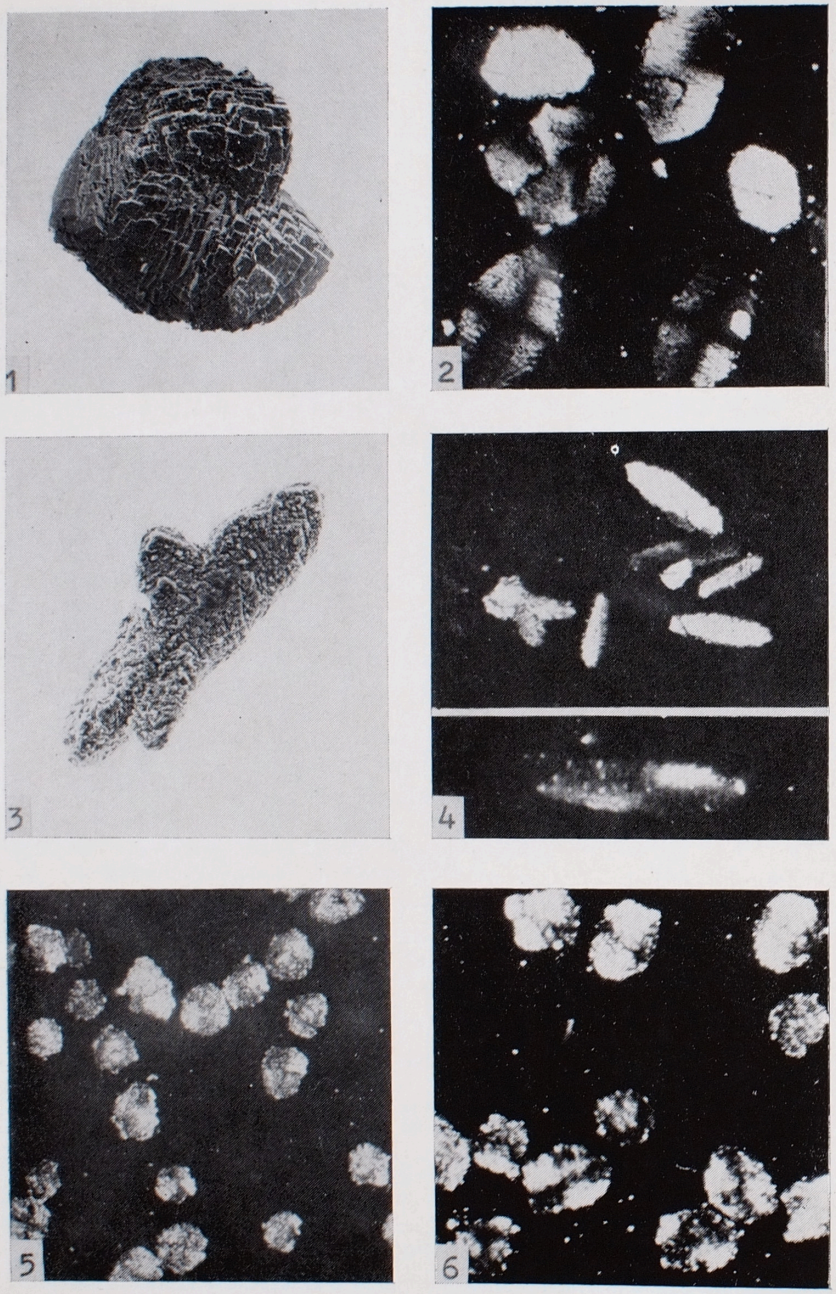

Tadeusz WIESER — Manganiferous carbonate micronodules of the Polish Carpathians Flysch deposits and their origin

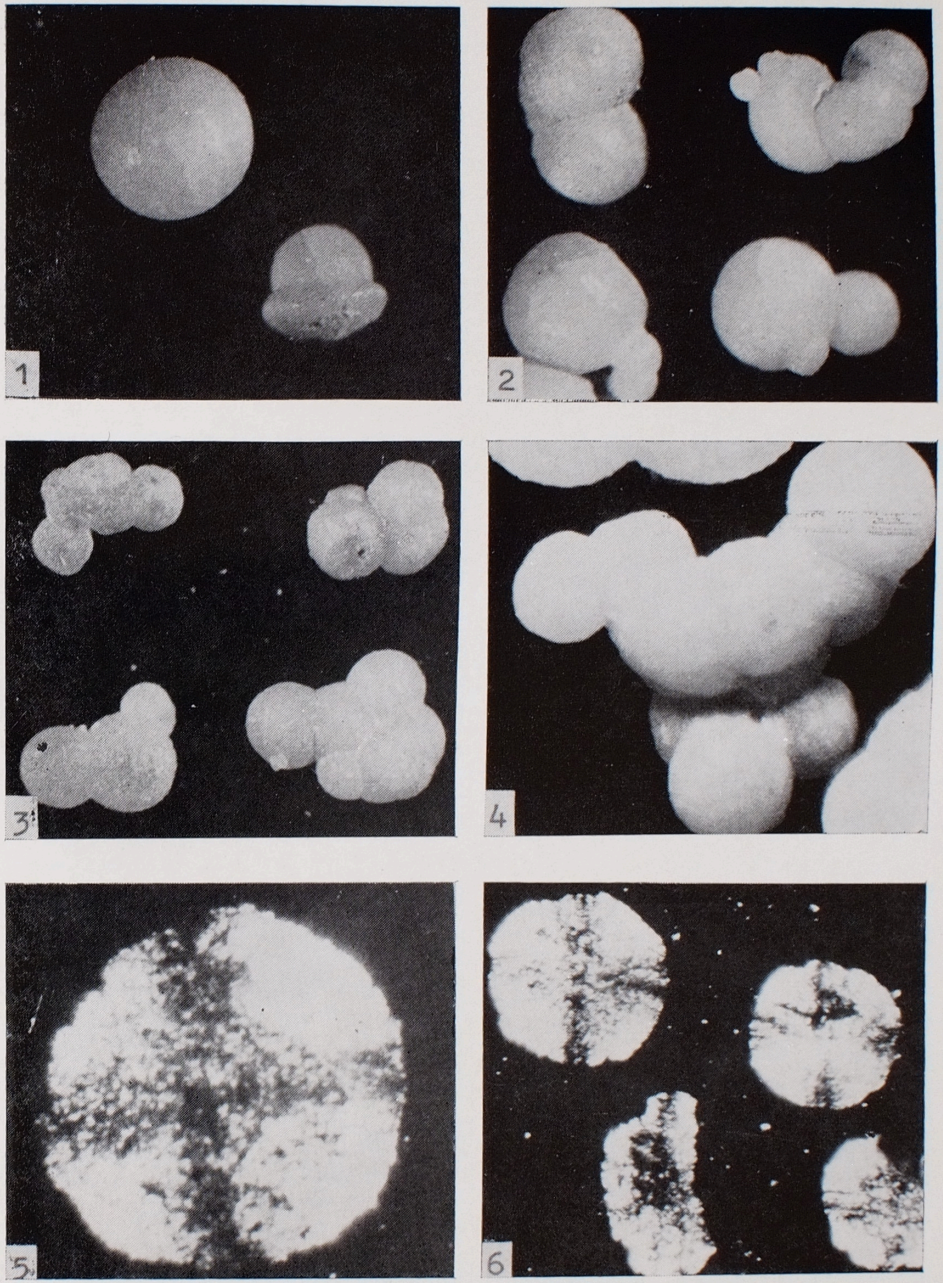

Tadeusz WIESER — Manganiferous carbonate micronodules of the Polish Carpathians Flysch deposits and their origin